applied sciences

IMPACT FACTOR 2.7

CITESCORE 4.5

Article

A New Traffic System on Driver Sensitivity and Safe Distance Headway

Zawar H. Khan and Ahmed B. Altamimi

MDPI

https://doi.org/10.3390/app132011262

applied sciences

MDPI

Article

A New Traffic System on Driver Sensitivity and Safe Distance Headway

Zawar H. Khan [1,*] and Ahmed B. Altamimi [2]

[1] Department of Electrical and Computer Engineering, University of Victoria, Victoria, BC V8P 5C2, Canada
[2] College of Computer Science and Software Engineering, University of Háil, Háil 55476, Saudi Arabia; altamimi.a@uoh.edu.sa
* Correspondence: khanz@uvic.ca

Abstract: A new macroscopic traffic system is devised that observes the transition distance between the vehicles and driver sensitivity during traffic evolution. The driver sensitivity in this system is based on the traversed time over a 200 m road section and speed (velocity). In addition, the proposed system considers the safe distance headway as the distance between vehicles changes. An analogy system for vehicle flow behavior is devised from a spring–mass system with changes in traffic. The proposed system can characterize traffic evolution for small and large changes in density. Furthermore, the changes in the travel of traffic rearwards during congestion and forward during smooth flow are dependent on driver sensitivity, transition distance, and safe distance headway. The proposed traffic system is hyperbolic. The Payne Whitham traffic system is based on uniform constant velocity for different conditions, which characterizes traffic evolution unrealistically. The proposed traffic system and the Payne Whitham system are assessed over a 2000 m circular road for large changes in density in two examples. Both the Payne Whitham and proposed traffic systems are numerically implemented with the first order centered scheme in Matlab. The discretization stability of both systems is enforced with the Courant–Friedrich–Levy (CFL) condition. The proposed system with lower driver sensitivity evolves with larger changes, whereas the proposed system with larger density has smaller changes in density and velocity. The simulation results showed that the traffic evolution with the proposed system is more appropriate than with the Payne Whitham system.

Keywords: macroscopic traffic system; driver sensitivity; safe distance headway; PW traffic system; hyperbolicity; numerical stability

Citation: Khan, Z.H.; Altamimi, A.B. A New Traffic System on Driver Sensitivity and Safe Distance Headway. *Appl. Sci.* **2023**, *13*, 11262. https://doi.org/10.3390/app132011262

Academic Editors: Luís Picado Santos and Junhong Park

Received: 17 July 2023
Revised: 6 October 2023
Accepted: 11 October 2023
Published: 13 October 2023

1. Introduction

Due to rapid traffic urbanization, congestion is a frequent problem on road networks. Traffic transition is the adjustment of vehicles to the following conditions when changes are noticeable. As the number of vehicles grows, stop and go traffic increases, that is, frequent transition in traffic occurs. It is significant to characterize traffic transition to alleviate traffic congestion [1]. This can improve travel time, reduce pollution, utilize the traffic infrastructure efficiently, and increase the comfort level of drivers. The transitions are dependent on the allowable distance between vehicles to prevent traffic accidents. This allowable distance is known as safe distance headway. As the safe distance headway increases, traffic has the tendency to adjust, which causes transition. To prevent accidents, the safe distance headway should be maintained during transitions. Reduced safe distance headway causes accidents. This is an example of aggressive driver behavior. Ignoring the distance headway results in abrupt changes in speed. Consequently, smaller distance headway causes excessive acceleration and deceleration [2], which increases the vehicle emissions and ultimately results in large environmental pollution [3,4]. It is also one of the major causes of accidents [5,6].

Further, fuel consumption is also increased compared to with typical driver behavior [7]. Reduced distance headway causes tailgating, which results in rear-end collisions.

Twenty-five percent of road accidents are due to tailgating [8,9]. Further, driver sensitivity impacts the distance between the vehicles. With higher driver sensitivity, changes during transitions are quick, and vice versa for lower driver sensitivity. The sensitivity of new drivers is low, and they perceive conditions with delayed response [10] as compared to experienced drivers. This causes longer delays and smaller distance headway. Further, during night time, the driver sensitivity of an experienced driver is reduced by 35% [11]. Driving with reduced sensitivity results in accidents [12,13]. The traversed time over a road segment determines the traffic changes and congestion [14]. This is an important parameter to be considered by urban planners to predict traffic conditions on a road network [15]. During congested periods, longer traversed time occurs with variable velocity. However, during smooth flow, the traversed time is smaller, traffic changes are negligible, and the tendency of road accidents is reduced. It is imperative to consider the safe distance headway, driver sensitivity, and traversed time during transitions to reduce accidents and effectively characterize a traffic system that can appropriately predict traffic evolution.

The most widely used traffic systems are microscopic and macroscopic. Microscopic systems consider vehicle behavior in the near vicinity [16,17]. For a larger number of vehicles, the mathematical details of drivers become complex, and is difficult to derive the theoretical laws as compared to macroscopic systems [18]. Macroscopic traffic systems consider the average traffic temporal and spatial evolution [19]. The macroscopic systems consider the density and velocity of a group of vehicles. This makes these types of systems independent from the number of vehicles, and it is easier to theoretically derive the system. The macroscopic systems are composed of a partial differential system with a number of traffic variables that consider the traffic physics and have realistic impact on the evolution.

Newell devised a microscopic traffic system in 1961 to characterize transitions during congestion [20]. The velocity of this system is impacted by distance headway. In other words, faster velocity is a result of larger distance headway and, conversely, slower velocity occurs for a smaller distance headway. However, this system ignores the driver perception of conditions. Bando et al. proposed that the changes in velocity are due to the variation in traffic density [21]. Further, this system also introduced driver sensitivity as a constant, which is an unrealistic approach. However, as velocity does not follow the density changes, a uniform acceleration occurs for different conditions, which is inappropriate. This results in an unstable evolution that ignores the variations in the leading and following vehicles [22]. Helbing and Tilch devised a system that contemplates differences in velocity of the following conditions [23]. The shortcoming of this system is that it considers acceleration and deceleration in a short time, which is atypical for driver behavior. This system ignores the generalized driver behavior. Gipps proposed a realistic system based on driver response [24]. This system does not perform well for a different parameter range [16]. Treiber et al. devised the car following system such that traffic spatial and temporal evolution is more accurate than the other systems in the field [25,26] The parameters considered are based on traffic physics [16]. This system considers velocity and distance headway of the following vehicles [27,28]. The acceleration/deceleration exponent considered in this system cannot accurately characterize the traffic changes and, consequently, an inappropriate evolution is observed. In the literature, different traffic systems incorporated the practical considerations of driver reactions to perceptions ahead [29]. In [30,31], traffic systems incorporate the safety of drivers with a consideration to changes in velocity. This system results in accidents as distance headway reduces between vehicles at a faster speed.

Macroscopic traffic systems are mostly used due to their simplicity and computational inexpensive properties [32]. The first macroscopic traffic system was devised by Lighthill, Whitham, and Richards (LWR) [33,34]. This system is based on the law of conservation [35], can predict flow for negligible changes, and ignores driver behavior and traffic acceleration/deceleration. This system results in inappropriate behavior during traffic transitions [36,37]. To complement the LWR system shortcomings, Payne and Whitham (PW) developed a second macroscopic traffic system. This system includes driver response to conditions of traffic and acceleration/deceleration to adjust during

transitions [37–40]. The driver response adjusts to the changes in traffic density ahead, and acceleration/deceleration (stop and go traffic) is the consequence of changes. The driver adjustments with a constant velocity to conditions in the vicinity causes inappropriate traffic evolution [40]. That is, velocity occurs below zero and above the maximum limits during large transitions and is contradictory to the real conditions [41,42]. The PW traffic system shortcomings are complemented by improving the driving response with a smaller reaction time during transitions [43]. However, this system cannot predict large density changes. This system has been improved to maintain traffic speed within the maximum and minimum limits [44]. This system ignored congested density conditions [45]. In [46], the relaxation time τ is dependent on density. According to [36], forward conditions have an impact on traffic evolution such that changes in velocity should be at or below the aggregate velocity. The changes at transitions cannot disseminate at a higher speed than the average in PW type systems. This has been contradicted in [47] with the reason that vehicles speed at transitions can go higher than the average in vehicles clusters or during lane changes. This is not an unrealistic behavior, rather, it reflects practical traffic conditions. Zhang [40] complemented the shortcomings of PW type systems by incorporating the equilibrium speed gradient. However, this system ignores the transition distance and time during traffic adjustment. In other words, the time to align [48] and the distance headway to control a vehicle is ignored.

In 2003, Zhang developed a traffic system based on microscopic and macroscopic traffic properties. This system removes the traffic discontinuities with a second order spatial derivative of speed. This is a mathematical approach. Further, this system introduced a constant to effectively model driver anticipation [49]. Zhai et al. contemplated the road slope during traffic alignment with a constant driver sensitivity. This is an inadequate approach, as the driver is not constant for different traffic conditions and can provide unrealistic traffic prediction [18]. The forward looking effect is the perception of a driver to changes ahead. Whereas, with backward impact, a driver accelerates from the approaching vehicles behind to avoid accidents [50]. In 2008, Ge et al. [51] considered the backward and forward impact with a constant driver sensitivity. Both the effects are devised with two different velocity systems. In 2018, Wang et al. [52] developed a system that considers the backward looking effect in traffic. This system considers driver sensitivity with a constant greater than 0. According to this system, the speed during congestion reduces with a large driver sensitivity, whereas at a negligible driver sensitivity, the traffic follows average velocity. In 2023, Jafaripournimchahi et al. [53] developed a system for connected and autonomous vehicles for anticipation. This system considered headway and vehicle torque.

Based on the given literature, the variable driver sensitivity for changes in the distance headway at transition in the second order traffic flow system has not been characterized. Therefore, in this paper, the impact of changes in distance headway between vehicles and driver sensitivity is considered in devising the second order (two-equation) traffic system. In this paper, the main contributions are

1. The Payne Whitham system is improved. Unlike the constant A in the PW system, the changes in traffic transitions are based on the driver sensitivity, safe headway, and transition headway. This is significant, as the traffic evolution at transitions is influenced by these physical parameters. This evolution is rapid for larger driver sensitivity. Conversely, the evolution is slow for a larger distance headway and smaller sensitivity. Thus, the spatio-temporal traffic evolution with the proposed system comprehends driver sensitivity, transition distance, and safe distance headway. These parameters are based on the traffic physics.
2. The driver sensitivity is obtained from the data acquired over a 200 m road section. A regressive relation for velocity and traversed time is obtained, which helps in the driver sensitivity characterization. This is incorporated in the proposed system for accurate traffic evolution.
3. It has been proved that the proposed traffic system is hyperbolic. Unlike the PW system, the changes during congestion and smooth flow, respectively, down and up,

are comprehended by the changes in transition distance about the safe headway and driver sensitivity.

4. The proposed system is assessed with the PW traffic system over a 2000 m circular road. The transition in density is considered at multiple locations with large changes in density over a circular road. At a location, density is 1, that is, 100%; 1 denotes that a road is at full capacity. This is the worst traffic scenario, and a system with a minor deviation from traffic physics can provide the density above the maximum and velocity below 0. This evolution is inappropriate traffic characterization, and the system cannot characterize the realistic practical traffic conditions during congestion. The performance results in this paper demonstrate that proposed traffic system can appropriately characterize traffic evolution as it considers the traffic physics and practical parameters. The traffic velocity with the proposed system does not go below 0 or above the maximum. The traffic density stays within the employed range.

The velocity distribution is given in Section 2, and Section 3 gives proposed system. The hyperbolicity is demonstrated in Section 4. The performance results are detailed in Section 5, and conclusions are in Section 6.

2. The Equilibrium Velocity Based on Traversed Time

The velocity behavior of vehicles covering a 200 m straight road section with traversed time is given in Figure 1. The lane discipline is not followed in this road section. Eleven different vehicle types were observed, while the total vehicles recorded were 170 in 3 h. The road section has two lanes, with a lane width of 3.2 m. The minimum traversed time recorded is 10 s, which occurred at the maximum velocity of 20 m/s. The maximum traversed time recorded is 42 s, which occurred at the minimum velocity of 3.4 m/s. The average traversed time is 18.1 s, and the average speed is 14.0 m/s. The recorded velocity is plotted against the traversed time as shown in Figure 1. Velocity is 20 m/s when covering 200 m in 10 s. The speed logarithmically reduces to 10 m/s as traversed time increases to 20 s. As it grows to 37 s, the velocity reduces to 5.40 m/s.

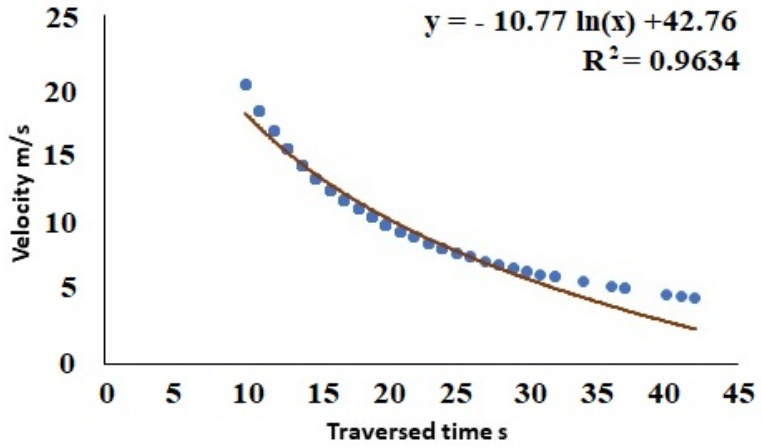

Figure 1. Velocity behavior based on the traversed time obtained from the experimental traffic data over 200 m.

The data fitness parameter, determination coefficient R^2, is based on velocity v and traversed time t, which is given as

$$R = \frac{n(\sum vt) - \sum v \sum t}{\sqrt{((n(\sum v^2 - (\sum v)^2))(n(\sum t^2 - (\sum t)^2)))}}, \quad (1)$$

where n denotes the number of observations in a dataset, and $\sum$ is the sum of variables. The other two parameters in regression for best fitness are mean absolute error (MAE) and mean squared error (MSE). A best fit model has the largest R^2, that is, closer to 1, and the

minimum MAE and MSE. The R^2, MSE, and MAE for logarithmic, exponential, and linear regressions are given in Table 1. The values of logarithmic regression are superior to the other types.

Table 1. Determination coefficient, mean squared errors, and mean absolute errors for best fitness of the data.

Description	Equation	Coefficient of Determination	Mean Squared Error (MSE)	Mean Absolute Error (MAE)
Logarithmic regression, traversed time	$-10.77 \ln t + 42.76$	0.963	1.218	0.904
Exponential regression, traversed time	$36.397exp^{-0.06t}$	0.960	1.283	1.022
Linear regression, traversed time	$-0.455t + 19.571$	0.855	3.798	1.836

The logarithmic characterization based on the behavior of velocity and traversed time obtained from the real data as shown in Figure 1 is given as

$$v(t) = -10.77\ln(t) + 42.76, \tag{2}$$

where $v(t)$ is the function of traversed time t; -10.77 is the slope of the regression line, whereas the line intercept is 42.76, which is the maximum time taken to cover 200 m section of the road. The largest R^2 = 0.96, minimum MSE = 1.218, and minimum MAE = 0.904 for (2) as shown in Table 1, which means that the logarithmic model is robust.

The logarithmic relation (2) shows that traffic velocity varies with the traversed time. That is, the velocity is large for a smaller traversed time and small for a larger traversed time, as shown in Figure 1. It is imperative to include the traversed time behavior in a macroscopic traffic model to accurately characterize the traffic evolution. Therefore, in this paper, traversed time is considered to devise the proposed traffic system.

3. Traffic Flow Modeling

Payne and Whitham (PW) devised a system that characterizes the driver response, acceleration/deceleration, and the traffic changes conservation for a large ideal road. This system includes two equations. The first equation considers the changes on an ideally long road with conserved (negligible) traffic changes. The second equation considers the driver response and the traffic acceleration. The driver response contemplates a constant, which dictates a uniform alignment of vehicles to different forward traffic conditions. The PW system is [37–40]

$$\begin{aligned} \rho_t + (\rho v)_x &= 0 \\ (\rho v)_t + \left(\rho v^2 + A^2\rho\right)_x &= \frac{v(\rho) - v}{\tau}, \end{aligned} \tag{3}$$

where t and x presents the partial spatio-temporal changes; ρ is density; v is velocity (speed); and $v(\rho)$ is the desirable equilibrium velocity. Relaxation time τ is required by the following vehicles to achieve $v(\rho)$ and align to the forward conditions; A is a uniform (constant) velocity at which drivers align to different traffic conditions. Traffic density is measured in vehicles per meter (veh/m). The average speed is measured in m/s, and the unit of τ is s. The unit of A is m/s. The expression (ρv) is the traffic flow and is measured in vehicles per second (veh/s). This is not an appropriate approach, as it ignores the transition distance and the distance headway between vehicles during the spatial and temporal traffic evolution. The following vehicles preserve the safe distance headway d_s with the forward vehicles in order to avoid from an unfortunate event. This behavior is analogous to a spring with a mass m attached. As a force is applied to the mass, the spring is extended, which stores potential energy to return to its stable position. This is an analogous scenario

with vehicle traffic. At a faster speed, vehicles have larger distances between vehicles. As the speed reduces, the distance between vehicles reduces, until it reaches safe distance headway d_s. That is, the vehicle transition distance d_t at different speeds fluctuates about d_s. As d_t increases relative to d_s, the vehicles accelerate, whereas the vehicles decelerate as the transition distance is smaller than d_s. Considering the analogous mass–spring and vehicle flow behavior, Hooke's law [54] for vehicle acceleration/deceleration α_t during the transition can be devised as

$$\alpha_t = \frac{k}{m}(d_t - d_s) \tag{4}$$

where m and k represent the spring mass and constant, respectively; $\eta = \frac{k}{m}$ is the sensitivity.

$$\alpha_t = \eta(d_t - d_s), \tag{5}$$

where η is analogous to the driver sensitivity during the traffic transition to align to the desirable velocity $v(\rho)$ of the forward vehicles. The traffic transition is based on the driver sensitivity η. For a small traversed time over a road section, the change to achieve the desirable velocity is large, and driver sensitivity is high. In contrast, for a large traversed time, the change to attain the desirable velocity is small, and, consequently, the driver sensitivity is low. The change to acquire the desirable speed depends on the speed behavior for the required traversed time over a road section. Therefore, the driver sensitivity is characterized with the second order time derivative of speed behavior to determine the change expected from (2). Then

$$\frac{\partial^2 v(t)}{\partial^2 t} = \frac{10.77}{t^2}. \tag{6}$$

For a normalized driver sensitivity, (6) becomes

$$\frac{1}{10.77}\frac{\partial^2 v(t)}{\partial^2 t} = \frac{1}{t^2}. \tag{7}$$

Then, the normalized driver sensitivity η from (7) takes form as

$$\eta = \frac{1}{t^2}. \tag{8}$$

As $\alpha_t = \frac{v_t}{\tau}$, where τ is the relaxation time required to align to forward conditions during transition; v_t is the traffic transition speed during alignment. Then, (5) from (8) is

$$v_t = \frac{(d_t - d_s)\tau}{t^2}. \tag{9}$$

This speed changes with the variation in the transition distance, traversed time, and driver reaction time. In contrast, the alignment to forward conditions considers a uniform speed, which is inappropriate and ignores the traffic evolution, whereas v_t is impacted by the traffic conditions. Substituting v_t from (9), the proposed system from (3) becomes

$$\begin{aligned} \rho_t + (\rho v)_x &= 0 \\ (\rho v)_t + \left(\rho v^2 + \left(\frac{(d_t - d_s)\tau}{t^2}\right)^2 \rho\right)_x &= \frac{v(\rho) - v}{\tau}. \end{aligned} \tag{10}$$

According to the proposed system (10), the spatial evolution is based on the driver sensitivity, transition distance, and the safe distance headway. In other words, the changes perceived on a road by a driver during traffic transitions depends on the sensitivity and maintenance of the safe distance headway. Unlike the traffic systems in the literature, the driver sensitivity is not a constant in the proposed system. When the transition distance

is comparable to the safe distance headway, there is no spatial evolution, and changes in traffic does not occur. For a larger difference between the transition distance and safe distance headway, large traffic changes are expected.

4. Model Hyperbolicity

The proposed traffic system (10) should satisfy the hyperbolicity condition, which says that the rate of change during transition for a congestion buildup should be smaller than the rate of change in free flow [55]. In other words, the free flow traffic evolution is at a higher rate than during congestion. The traffic dissemination is quick during free flow and is slow during congestion. This hyperbolicity property of the proposed traffic system should ensure that velocity fluctuates in a finite range of 0 and the minimum limit. To check the hyperbolicity, the conserved form of (10) for ρ and ρv is

$$\begin{aligned} \rho_t + (\rho v)_x &= 0 \\ (\rho v)_t + \left(\frac{(\rho v)^2}{\rho} + \left(\frac{(d_t - d_s)\tau}{t^2} \right)^2 \rho \right)_x &= \frac{v(\rho) - v}{\tau}. \end{aligned} \tag{11}$$

Equation (11) is in a quasi-linear form and is appropriate for the Jacobian matrix to acquire eigenvalues. The two variables in (11) are ρ and ρv. The spatial components are partially differentiated with ρ and ρv such that the spatial components are linearized. Then, the Jacobian matrix is

$$\begin{pmatrix} j_{11} & j_{12} \\ j_{21} & j_{22} \end{pmatrix}, \tag{12}$$

where $j_{11} = \frac{\partial}{\partial \rho}\rho$, $j_{12} = \frac{\partial}{\partial \rho v}\rho$, $j_{21} = \frac{\partial}{\partial \rho}\left(\frac{(\rho v)^2}{\rho} + \left(\frac{(d_t - d_s)\tau}{t^2} \right)^2 \rho \right)$, and $j_{22} = \frac{\partial}{\partial \rho v}\left(\frac{(\rho v)^2}{\rho} + \left(\frac{(d_t - d_s)\tau}{t^2} \right)^2 \rho \right)$. The Jacobian matrix of the proposed system (10) from (12) is

$$\begin{pmatrix} 0 & 1 \\ -v^2 + \left(\frac{(d_t - d_s)\tau}{t^2} \right)^2 & 2v \end{pmatrix}, \tag{13}$$

then the eigenvalues are

$$\begin{aligned} \lambda_1 &= v + \frac{(d_t - d_s)\tau}{t^2}, \\ \lambda_2 &= v - \frac{(d_t - d_s)\tau}{t^2}. \end{aligned} \tag{14}$$

Eigenvalues show that the proposed traffic system (10) is hyperbolic, as $\lambda_{1,2}$ are real and distinct. Further, the velocity fluctuations are dependent on $\frac{(d_t - d_s)\tau}{t^2}$, that is, for a larger traversed time, the expected traffic evolution is slower, whereas for a smaller traversed time, the expected traffic evolution is faster. The changes in the forward direction of traffic are disseminated at the rate λ_2. That is, the traffic changes in acceleration and deceleration in a smooth flow travel with the speed λ_2. The acceleration and deceleration traveling speed in the forward direction reduces with a higher driver sensitivity than with a lower driver sensitivity. In the rearward direction, the changes are disseminated at the rate λ_1. In other words, during congestion, the changes in acceleration and deceleration travel down the traffic with the speed λ_1. That is, the acceleration and deceleration traveling speed in the rearward direction is always greater than the average speed with changes in driver sensitivity. At $d_t = d_s$, the changes in both the forward and rearward directions travel with average speed v.

The PW system (3) Jacobian matrix from (12) is

$$\begin{pmatrix} 0 & 1 \\ -v^2 + A^2 & 2v \end{pmatrix}, \tag{15}$$

and the eigenvalues are

$$\begin{aligned} \lambda_1 &= v + A, \\ \lambda_2 &= v - A. \end{aligned} \tag{16}$$

Eigenvalues show that the PW traffic system (3) is hyperbolic, as $\lambda_{1,2}$ are real and distinct. Further, the velocity fluctuations are dependent on A, that is, traffic evolution is at a uniform constant rate, which is not appropriate and contradictory to the traffic physics. The traffic evolution with (10) changes as the transition distance, relaxation time, and traversed time changes. In other words, the proposed traffic system (10) considers the traffic system, and the traffic evolution is impacted by the conditions.

Numerical Stability

For the proposed and PW traffic systems, the first order centered (FORCE) scheme [56] is used. This scheme can approximate impulsive changes and can accurately estimate traffic evolution. Therefore, this is used for the solution of traffic systems. This merges Richtmyer and Lax–Friedrichs schemes to accurately asses second order traffic systems. The benefit of the FORCE scheme is its lower computational cost and easy implementation compared to the ROE scheme [57]. For the stability of this numerical scheme employed to a hyperbolic traffic system [58], the spatial size of a road segment Δx should be larger than the temporal step Δt. That is, the space acquired by the traffic in temporal steps should be smaller than the spatial steps. This is mandatory to ensure that the solution should not grow or decay due to hyperbolic traffic system nature. Therefore, the Courant–Friedrich–Levy (CFL) condition [17,59] is employed, and is given as

$$\max |\lambda| \frac{\Delta t}{\Delta x} \leq 1. \tag{17}$$

This is the maximum spatial road segment that can be covered in a temporal step. For numerical accuracy and stability, the distance covered during the traffic evolution over the temporal step should be smaller than a spatial road segment, therefore

$$\Delta t \leq \frac{\Delta x}{\max |\lambda|}. \tag{18}$$

For the proposed traffic system, the maximum eigenvalue from (14) at maximum velocity is

$$\max |\lambda| = \left| v_m + \frac{(d_t - d_s)\tau}{t^2} \right|, \tag{19}$$

and the corresponding stability condition is

$$\Delta t < \frac{\Delta x}{\max \left| v_m + \frac{(d_t - d_s)\tau}{t^2} \right|}. \tag{20}$$

For the PW traffic system, the maximum from (16) is

$$\max |\lambda| = |v + A|, \tag{21}$$

and the corresponding stability condition is

$$\Delta t < \frac{\Delta x}{\max |v + A|}. \tag{22}$$

If (20) and (22) are guaranteed in the numerical solution, the performance results of both traffic systems in the next section will be stable.

5. Performance Evaluation

The performance of the PW and the proposed system is analyzed over a 2000 m circular road in examples 1 and 2. Periodic boundary conditions are implemented in MATLAB 9.7 to consider a circular road in both the examples. The desirable velocity is the Greenshields equilibrium velocity [60] and is

$$v(\rho) = v_m\left(1 - \frac{\rho}{\rho_m}\right), \tag{23}$$

where ρ_m presents maximum normalized density, and v_m is the maximum velocity or the speed limit of a road. Equation (23) presents a hyperbolic fundamental flow. That is, flow increases for a small density and decreases when traffic is congested [61–64]. In microscopic traffic models, the relaxation time varies as the behavior of each driver is considered [65]. In macroscopic models, the average behavior is considered, therefore the relaxation time for both examples is 2 s.

5.1. Example 1

The time for both system simulations is 100 s. The maximum velocity is 0.964 m/s [54]; d_t is 8 m, and $d_s = 2$ m [65–67]. The velocity constant for the PW model is 25 m/s. The spatial road step for the proposed and PW systems is 5 m. For the proposed model, as per given condition (20), the maximum temporal time step is 4.99 s. Whereas per condition (22), the maximum temporal step for the PW model is 0.19 s. To ensure this CFL stability condition, the temporal step is chosen as 0.01 s, which is less than 4.99 s and 0.19 s, respectively, for the proposed and PW models [59]. That is, the speed of iteration is faster than the traffic speed in a temporal step. The traversed time is 18.08 s, which gives a driver sensitivity of 0.0031 s^{-2} as shown in Table 2.

The initial density over 2000 m at 0 s for the performance results in example 1 is

$$\rho_0 = \begin{cases} 0.01 & \text{for } x \leq 600 \\ 0.3 & \text{for } x \leq 1000 \\ 1 & \text{for } x \leq 1500 \\ 0.5 & \text{for } x \leq 2000. \end{cases} \tag{24}$$

The changes in density distribution ρ_0 represent the traffic transition. The initial transitions are at 600 m, 1000 m, and 1500 m.

Table 2. Traffic parameters.

Parameter	Value
Time of simulation	100 s
Length of the circular road	2000 m
Maximum velocity	0.964 m/s
Minimum velocity	0 m/s
Velocity constant	$A = 25$ m/s
Equilibrium velocity	$v(\rho)$ = Greenshields
Maximum normalized density	$\rho_m = 1$
Minimum normalized density	$\rho_m = 0$
Temporal step	0.1 s
Spatial road step	5 m
Relaxation time	$\tau = 2$ s
Safe distance headway	$d_s = 2$ m
Transition distance	$d_t = 8$ m
Traversed time	$t = 18.08$ s
Driver sensitivity	$\eta = \frac{1}{t^2} = 0.0031$ s^{-2}

The proposed traffic system velocity over 2000 m at 1 s, 50 s, and 100 s is depicted in Figure 2. At 1 s, 0.57 m/s is at 0 m, which at 40 m grows to 0.968 m/s and continues up to 470 m. It drops to 0.7 m/s from 500 m/s, which continues up to 1000 m. A velocity of 0 m/s is at 1030 m, which continues up to 1500 m. At 50 s, it is 0.68 m/s, which, at 230 m, grows to 0.96 m/s. The speed at 700 m drops to 0.7 m/s and at 1080 m drops to 0 m/s. At 100 s, it is 0.65 m/s, which, at 270 m, grows to 0.96 and at 680 m drops to 0.7 m/s. The speed at 1200 m further drops to 0.014 m/s. It grows at 855 m to 0.51 m/s, which at 1994 m grows to 0.64.

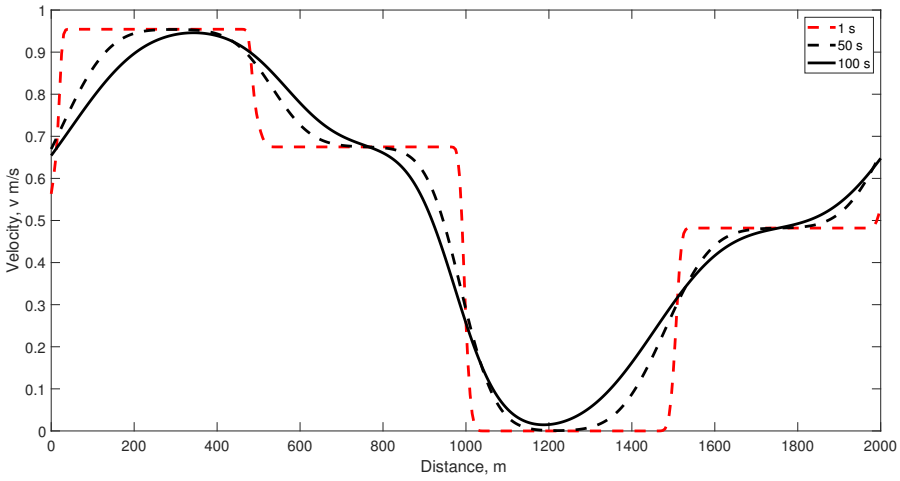

Figure 2. Velocity with the proposed system on a 2000 m circular road with a driver sensitivity of 0.0031 s^{-2}.

The proposed system traffic velocity behavior over 2000 m for 100 s is shown in Figure 3. The velocity behavior shows that the velocity remains within the bounds both spatially and temporally. Speed (velocity) behavior is correspondingly based on the density behavior, as shown in Figures 4 and 5. As the density grows, the velocity drops. Conversely, as the density decays, the velocity increases. That is, the proposed system behaves according to the behavior of the desired equilibrium velocity, which is realistic and adequate.

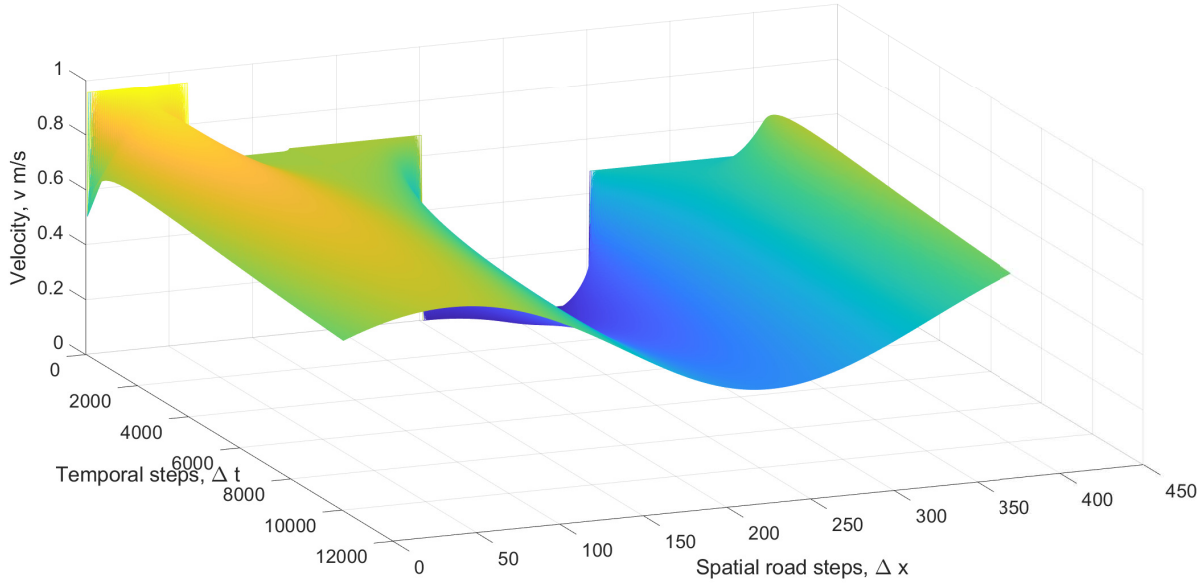

Figure 3. Velocity with the proposed system on a 2000 m circular road with a driver sensitivity of 0.0031 s^{-2}.

The corresponding proposed traffic system density of the velocity as demonstrated in Figures 2 and 3 over 2000 m at 1 s, 50 s, and 100 s is depicted in Figure 4. At 1 s, 0.21 is at 0 m, which drops to 0.01 m/s at 30 m, and stays constant up to 470 m. It grows to 0.3 at 521 m, which further grows to 1 at 1030 m. Density drops to 0.5 at 1520 m, and stays constant up to 1970 m. At 50 s, it is 0.3 at 0 m, which drops to 0.01 at 300 m. It grows to 0.3 at 700 m. The density further grows to 1 at 1200 m, and further reduces to 0.3 at 1700 m. At 100 s, it is 0.31 at 0 m, which drops to 0.01 at 350 m. The density further increases to 0.3 at 700 m, reaches 0.98 at 1200 m, and drops to 0.3 at 1850 m.

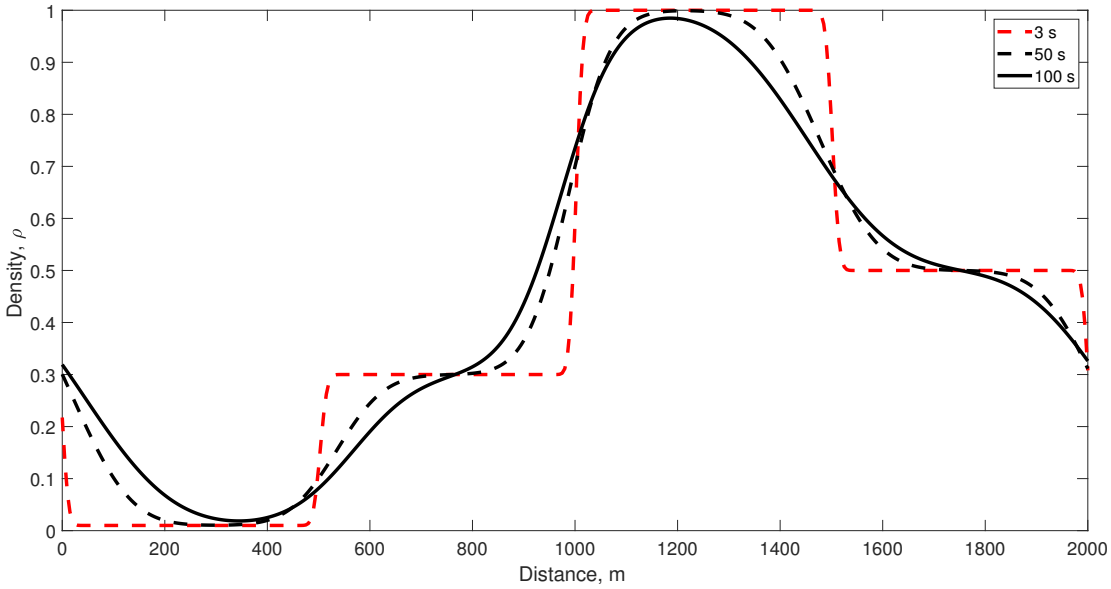

Figure 4. Density with the proposed system on a 2000 m circular road with a driver sensitivity of 0.0031 s^{-2}.

The proposed traffic system density on a 2000 m circular road for 100 s is demonstrated in Figure 5. The density stays within the defined limits over the temporal and spatial road steps. The traffic density at 95 s at 360 m is 0.017, whereas at 1200 m, it is 0.98 and drops to 0.32 at 2000 m.

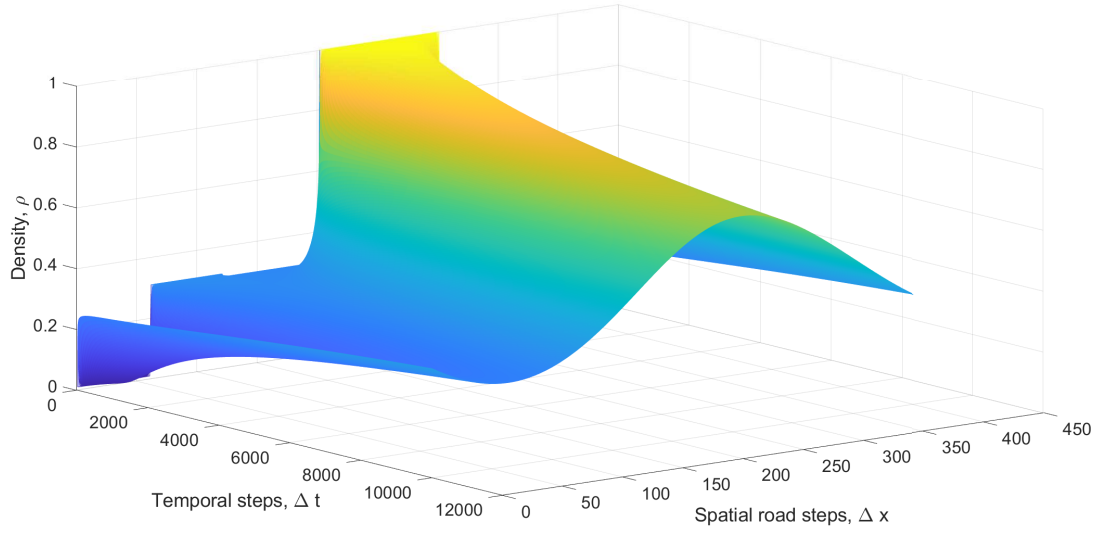

Figure 5. Density with the proposed system on a 2000 m circular road with a driver sensitivity of 0.0031 s^{-2}.

The PW traffic system density on a 2000 m circular road at 1 s, 50 s, and 100 s is depicted in Figure 6. At 1 s, the density is 0.211 at 0 m, which drops to 0.01 m/s at 30 m, and stays constant up to 430 m. The density grows to 0.3 at 31 m, which further grows to 1 at 1030 m. The density drops to 0.5 at 1030 m. At 50 s, it is 0.27 at 0 m, which drops to 0.23 at 340 m. The density further grows to 0.8 at 1250 m and further reduces to 0.27 at 2000 m. At 100 s, it is 0.34 at 0 m, which drops to 0.24 at 300 m. The density further grows to 0.8 at 1250 m and drops to 0.27 at 2000 m.

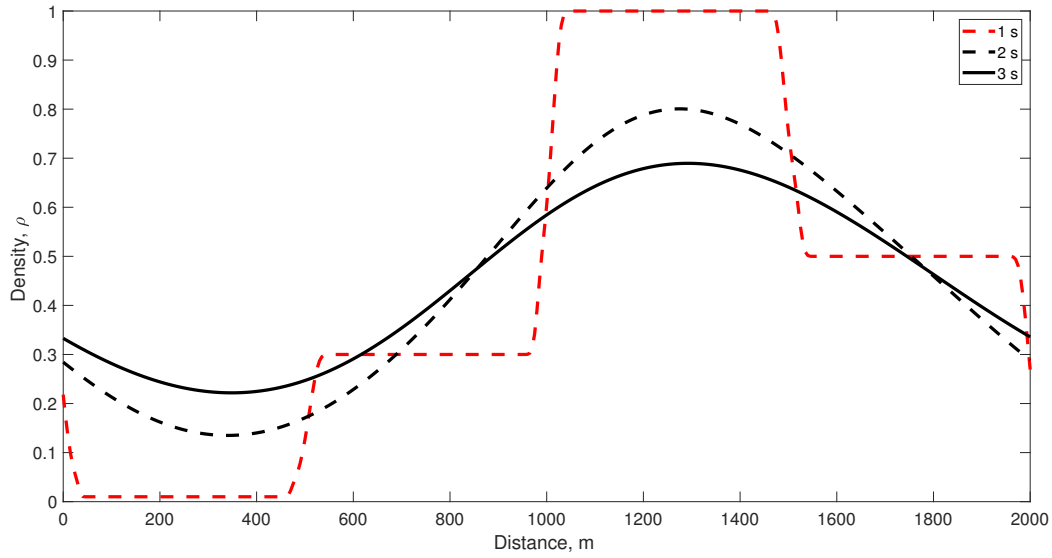

Figure 6. Density with the PW traffic system on a 2000 m circular road with $A = 25$ m/s.

The PW traffic system density on a 2000 m circular road for 100 s is demonstrated in Figure 7. The density stays within the defined limits over the temporal and spatial road steps. However, the traffic transition from higher to lower density disseminates very quickly, which is not realistic as compared to the proposed system traffic density behavior as given in Figure 5.

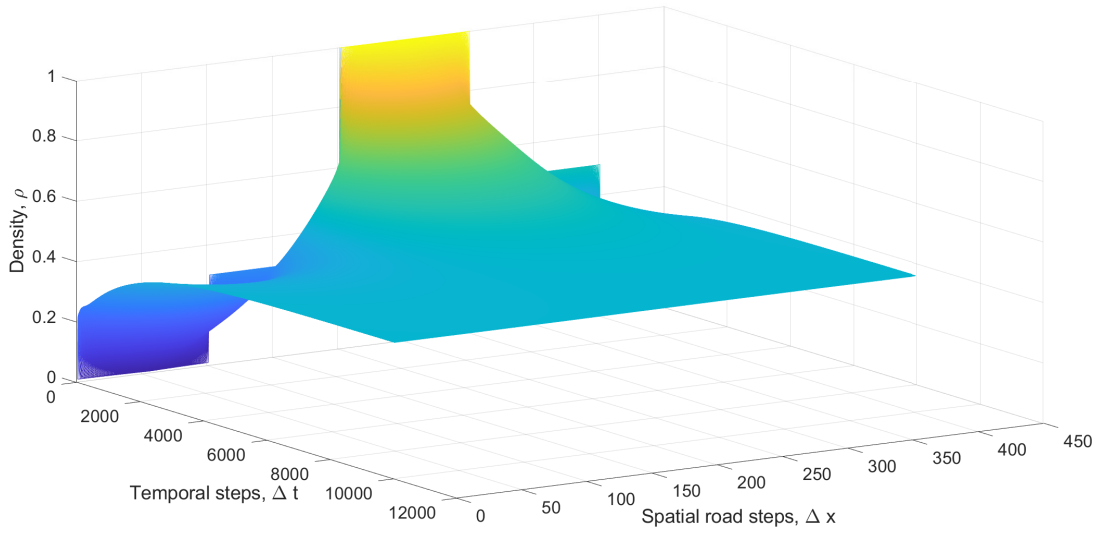

Figure 7. Density with the PW traffic system on a 2000 m circular road with $A = 25$ m/s.

The corresponding PW traffic system velocity of density given in Figures 6 and 7 on a 2000 m circular road at 1 s, 50 s, and 100 s is depicted in Figure 8. At 1 s, the velocity

is 25.5 m/s at 30 m, which drops to −21 m/s at 440 m. The velocity is 0.955 from 525 m/s to 925 m. It is as low as −7 m/s at 1000 m and as high as −5 at 1500 m. At 50 s, it is 2.4 m/s, which grows to 2.7 m/s at 160 m. The velocity grows to −1.25 m/s at 650 m, and further rises to 2.4 m/s at 2000 m. At 100 s, it is 1.7 m/s, which drops to −0.6 at 700 m, and further grows to 1.7 m/s at 2000 m.

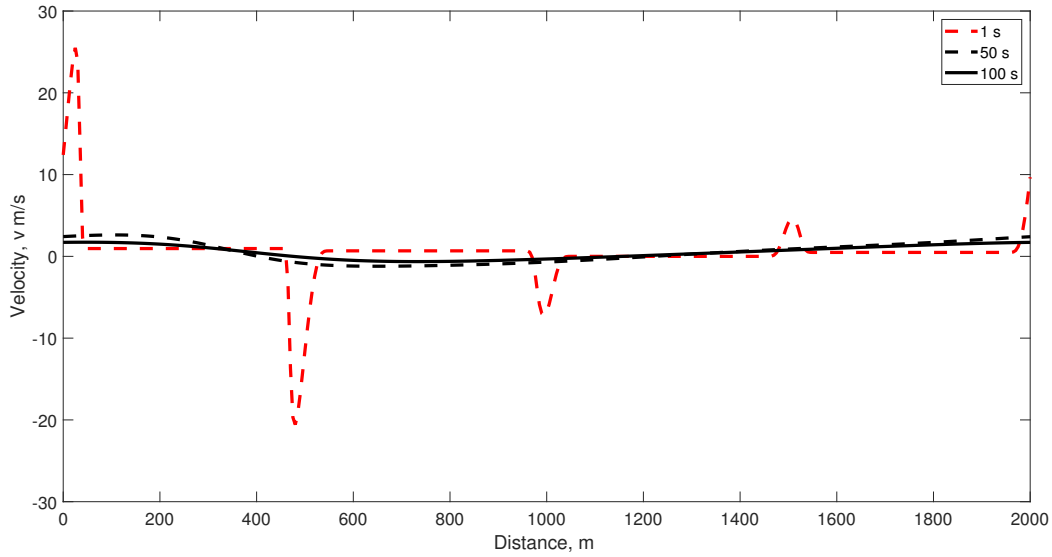

Figure 8. Velocity with the PW system on a 2000 m circular road with $A = 25$ m/s.

The PW velocity evolution on a 2000 m circular road for 100 s is demonstrated in Figure 9. As expected, the traffic velocity is not within the range of the minimum 0 m/s and maximum 0.968 m/s. The velocity goes below 0 m/s until it reaches −20 m/s and stays negative until 100 s. The velocity above the maximum goes to 25.5 m/s at 1 s. The velocity stays above the maximum until 100 s. The PW traffic system velocity is not within the limits.

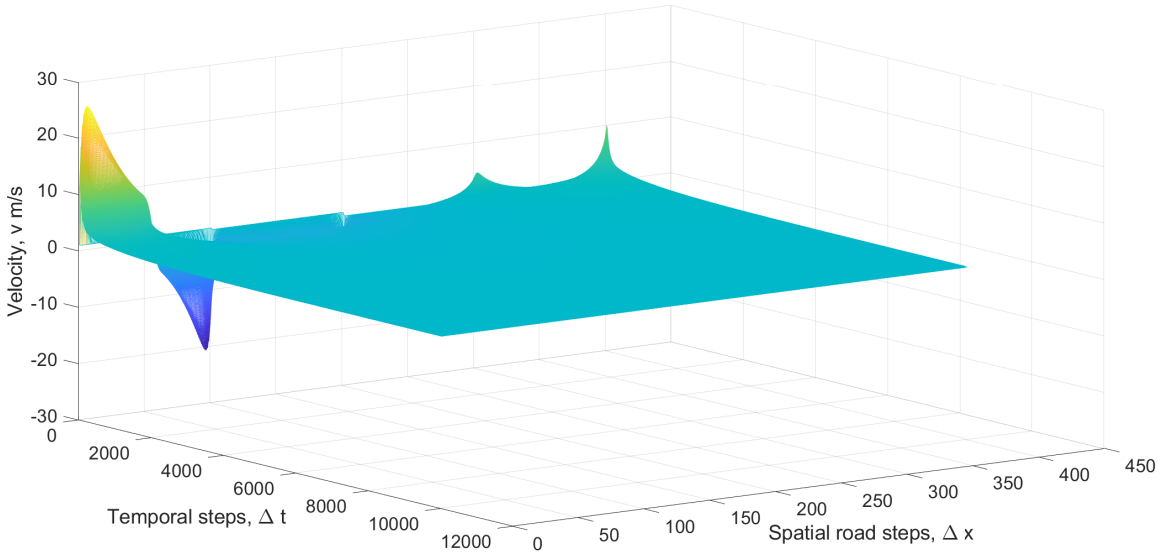

Figure 9. Velocity with the PW system on a 2000 m circular road.

5.2. Example 2

The proposed system is analyzed with traversed time during transition as 1 s and 20 s, which, respectively, gives the driver sensitivity as 1 s^{-2} and 0.0025 s^{-2} as shown in Table 3. The temporal step is 0.2 s, with the spatial road step chosen as 14 m to satisfy the CFL conditions [59]. The value of d_t is 18 m. The maximum and minimum velocity, respectively, are 25 m/s and 0 m/s [17]. The total simulation time for example 2 is 200 s. The initial density distribution ρ_0 over 2000 m at time $t = 0$ for the performance results in example 2 is

$$\rho_0 = \begin{cases} 0.15 & \text{for } x \leq 300 \\ 0.8 & \text{for } x \leq 600 \\ 0.3 & \text{for } x \leq 1000 \\ 0.8 & \text{for } x \leq 1500 \\ 0.2 & \text{for } x \leq 2000 \end{cases} \tag{25}$$

The changes in density distribution (25) presents the traffic transition. This distribution has transitions at 300 m, 600 m, 1000 m, and 1500 m.

Table 3. Traffic parameters.

Parameter	Value
Simulation time	200 s
Length of the circular road	2000 m
Maximum velocity	25 m/s
Minimum velocity	0 m/s
Equilibrium velocity	$v(\rho)$ = Greenshields
Maximum normalized density	$\rho_m = 1$
Minimum normalized density	$\rho_m = 0$
Temporal step	0.2 s
Spatial road step	14 m
Relaxation time	$\tau = 2$ s
Safe distance headway	$d_s = 2$ m
Transition distance	$d_t = 18$ m
Traversed time	$t = 20$ s
Driver sensitivity η	$\frac{1}{t^2} = 0.0025\ s^{-2}$
Traversed time	$t = 1$ s
Driver sensitivity η	$\frac{1}{t^2} = 1\ s^{-2}$

Figure 10 depicts the density of the proposed system on a 2000 m circular road with 0.0025 s^{-2} and 1 s^{-2} driver sensitivity at 0.2 s, 12 s, 100 s, and 200 s. With 0.0025 s^{-2}, at 0.2 s, the density is 0.15 from 0 m to 300 m, whereas from 301 m to 600 m, it is 0.8. From 601 m to 1000 m, it is 0.3, whereas the density from 1001 m to 1500 m is 0.8. At 12 s, the density bounds between 0.17 and 0.92. At 0 m, it is 0.2, and it is 0.17 at 285 m. The density grows to 0.89 at 390 m, and it drops to 0.29 at 800 m. This grows to 0.92 at 1040 m, which then drops to 0.8 at 1200 m and stays contant up to 1300 m. The density drops to 0.18 at 1800 m. At 100 s, the density bounds between 0.29 and 0.81. At 0 m, it is 0.4, and it is 0.29 at 635 m. The density grows to 0.81 at 785 m and drops to 0.5 at 1000 m. This grows to 0.6 at 1190 m and then drops to 0.5 at 1500 m. At 200 s, it is between 0.47 and 0.6. At 0 m, it is 0.45, and it is 0.4 at 900 m. The density grows to 0.56 at 1050 m and then grows to 0.6 at 1280 m, but then drops to 0.47 at 1500 m. With 1 s^{-2}, at 0.2 s, it is shown in Figure 10 that the density behavior with the proposed system is the same as with the driver sensitivity 0.0025 s^{-2}. At 12 s, the density is between 0.19 and 0.77. At 0 m it is 0.2, and it is 0.19 at 150 m. The density grows to 0.6 at 410 m, whereas it drops to 0.37 at 800 m. This grows to 0.77 at 1200 m and then drops to 0.2 at 2000 m. At 100 s, the density bounds between 0.38 and 0.51. At 0 m, it is 0.42, and it is 0.38 at 500 m. The density grows to 0.51 at 1000 m, whereas it drops to 0.4 at 1500 m. This further drops to 0.4 at 2000 m. At 200 s, the density bounds between

0.43 and 0.47. At 0 m, it is 0.45, and it is 0.43 at 600 m. The density grows to 0.47 at 1500 m, whereas it drops to 0.46 at 2000 m. Figure 10 demonstrates that the variation in density with 0.0025 s^{-2} is larger than with 1 s^{-2} and shows appropriate evolution.

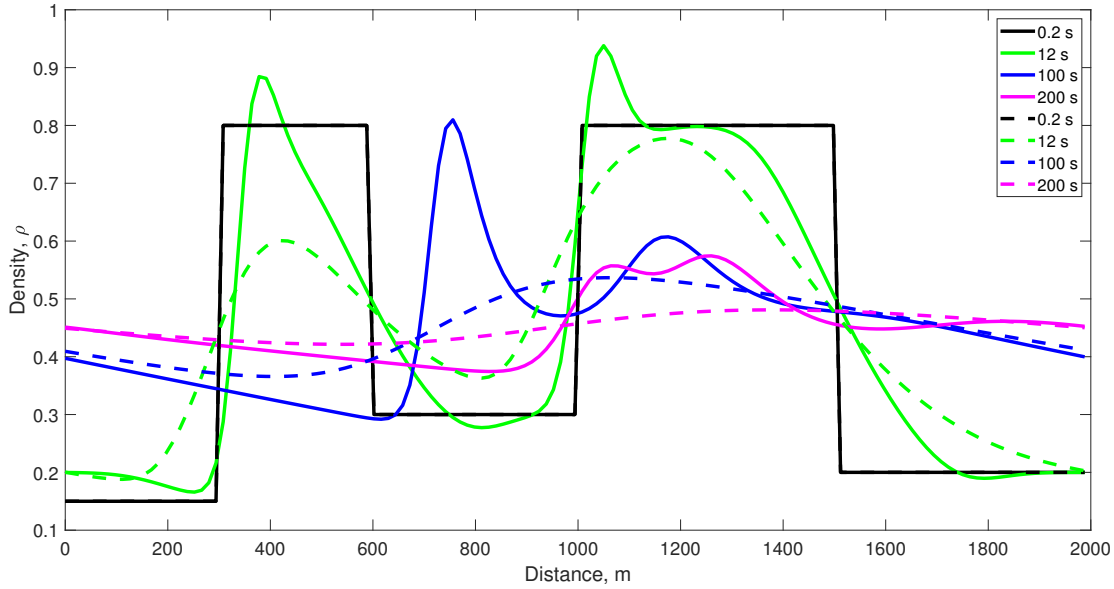

Figure 10. Traffic density behavior with the proposed system on a 2000 m circular road. The solid lines represent the proposed system behavior with the driver sensitivity 0.0025 s^{-2}at 0.2 s, 12 s, 100 s, and 200 s. The dotted lines represent the proposed system behavior with the driver sensitivity 1 s^{-2} at 0.2 s, 12 s, 100 s, and 200 s.

For 1 s^{-2}, at 0.2 s, Figure 11 shows that the velocity behavior with the proposed system is the same as with the driver sensitivity of 0.0025 s^{-2}. At 12 s, it is bounded from 5.7 m/s to 22.3 m/s. At 0 m, it is 22.3 m/s, and it is 10 m/s at 308 m. The velocity drops to 8.8 m/s at 364 m, whereas it grows to 18 m/s at 784 m. This drops to 5.7 m/s at 1134 m and then grows to 21.7 m/s at 1792 m. At 100 s, the velocity is bounded from 12.4 m/s to 17.2 m/s. The velocity at 0 m is 16.1 m/s, and it is 17.2 m/s at 392 m. The velocity drops to 12.4 m/s at 982 m, whereas it grows to 14 m/s at 1540 m. This further grows to 16 m/s at 2000 m. At 200 s, it is bounded from 13.97 m/s to 15.5 m/s. At 0 m, it is 15 m/s, and it is 15.5 m/s at 630 m. The velocity drops to 13.97 m/s at 1302 m, whereas it grows to 14.7 m/s at 2000 m. For 0.0025 s^{-2}, at 12 s, velocity is bounded from 3.8 m/s to 22.5 m/s. At 0 m, it is 21.6 m/s, and it is 22.5 m/s at 252 m. The velocity drops to 4.8 m/s at 392 m, whereas it grows to 18 m/s at 800 m. This drops to 3.8 m/s at 1078 m, which then grows to 5.4 m/s at 1200 m and stays constant up to 1300 m. The velocity grows to 21.7 m/s at 1800 m. At 100 s, it is bounded from 6.7 m/s to 19 m/s. The velocity at 0 m is 16.1 m/s, and it is 19 m/s at 635 m. The velocity drops to 6.7 m/s at 775 m, whereas it grows to 14 m/s at 1000 m. This grows to 14.5 m/s at 1652 m and then further grows to 16 m/s at 2000 m. At 200 s, it is bounded from 12 m/s to 16.84 m/s. At 0 m, it is 14.9 m/s, and it is 16.84 m/s at 868 m. The velocity drops to 12.2 m/s at 1092 m, whereas it drops to 12 m/s at 1204 m, grows to 14.8 m/s at 1653 m, and stays approximately uniform up to 2000 m. Figure 11 demonstrates that the variation in velocity with 0.0025 s^{-2} is larger than with 1 s^{-2} and shows appropriate evolution.

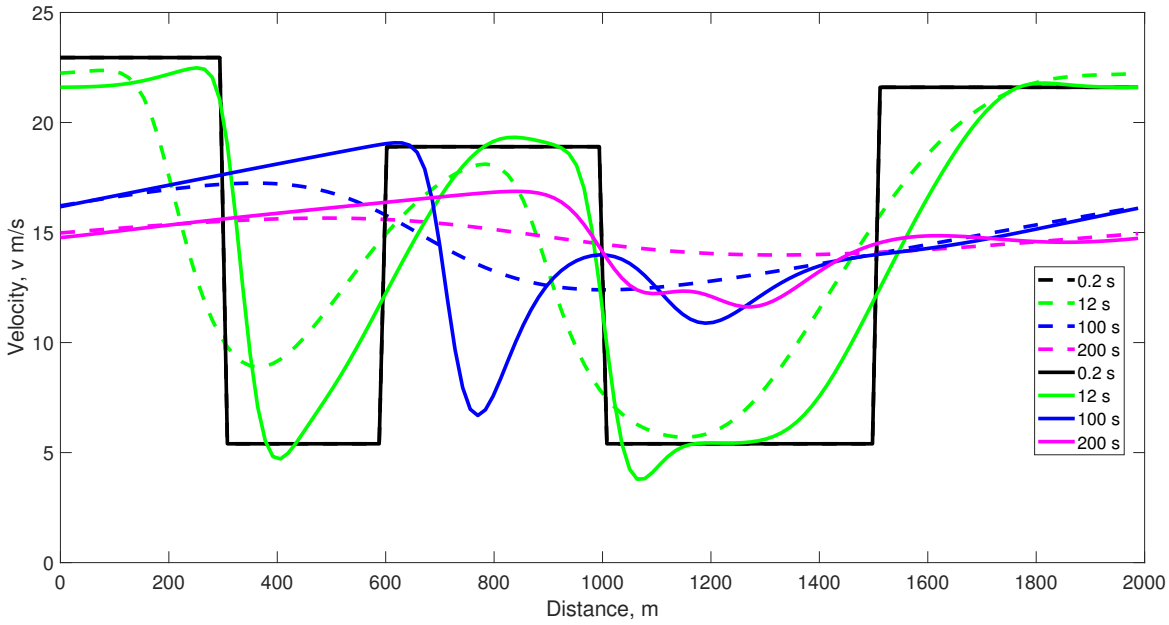

Figure 11. Traffic velocity behavior with the proposed system on a 2000 m circular road. The solid lines represent the proposed system behavior with the driver sensitivity of 0.0025 s^{-2} at 0.2 s, 12 s, 100 s, and 200 s. The dotted lines represent the proposed system behavior with the driver sensitivity of 1 s^{-2} at 0.2 s, 12 s, 100 s, and 200 s.

6. Discussion of Results

Figures 2–5 show that the density and velocity with the proposed system are within the employed range for the worst case scenario of maximum density 1. The traffic adjustment during the density and velocity changes are according to the employed conditions. That is, as the density grows, velocity drops, and the opposite behavior of velocity is observed with a decay in the density on the road. In this illustration, the driver sensitivity is 0.0031 s^{-2} during transitions at multiple locations on a 2000 m circular road.

Conversely, with the PW traffic system, it is observed in Figures 8 and 9 that the velocity does not evolve according to the density behavior as depicted in Figures 6 and 7, although the simulations conditions for both the PW and proposed traffic systems are the same. The velocity with the PW traffic system goes negative and above the maximum velocity limit. The maximum velocity observed with PW traffic system is 25.5 m/s, which is inaccurate, as the maximum allowable velocity is 0.964 m/s. The minimum velocity observed is -20 m/s, although the minimum allowable velocity is 0 m/s. As expected, the traffic velocity is unrealistic as the driver behavior adjusts to the following conditions uniformly. In addition, traffic adjustment during the density and velocity transition is not based on traffic physics.

Figures 10 and 11 show the proposed traffic system evolution with the driver sensitivities of 0.0025 s^{-2} and 1 s^{-2} for 200 s. The results show that the traffic evolves differently at 0.0025 s^{-2} than with 1 s^{-2}. Figure 10 show that the velocity evolves more quickly with 1 s^{-2} than with 0.0025 s^{-2}. As expected, the smaller traversed time during transition aligns more quickly than with a larger traversed time. A sensitivity of 1 s^{-2} represents that the flow is smooth and has smaller tendencies for larger velocity changes. Whereas with 0.0025 s^{-2}, the driver takes longer during transitions to align. This is a presentation of congested flow and has tendencies for larger changes in velocity. Figure 11 shows that the density with 1 s^{-2} aligns quickly. The changes in density are smaller than with 0.0025 s^{-2}. The density with 0.0025 s^{-2} has larger changes as expected than with 1 s^{-2}. The density for both of the driver sensitivities is within the employed range of the maximum 1 and 0. The velocity also stays within the bounds. The velocity changes with the proposed traffic system follow

the changes in density and have the tendency to acquire the Greenshields velocity–density behavior. The realistic and appropriate behavior of the proposed traffic system is due to the appropriate characterization of driver behavior based on traffic physics. That is, the proposed system considers the traffic density, transition distance, and distance headway during transitions.

The inaccurate and inappropriate traffic evolution with the PW traffic system is due to the traffic characterization as a constant at traffic transitions. This shows that, unlike the PW traffic system, the proposed traffic system is more robust. The proposed model is applicable to the traffic flow where lane discipline is not followed. This can produce better results in different road conditions, as the performance results were evaluated for the worst traffic conditions in a circular road, where the traffic changes remain in the circle. These changes are more prone to further larger changes and cause excessive acceleration and deceleration. In addition, the traffic conditions are more vulnerable to traffic accidents. This also causes excessive vehicle emissions due to the frequent occurrence of acceleration and deceleration. However, the proposed model mitigates traffic conditions and improves public safety, which is significant. The emissions are reduced as the acceleration and deceleration are reduced due to smaller changes as shown in the performance results.

The proposed system improves upon the LWR model [33,34], as the latter only considers the idealized traffic conditions. The Zhang model only considered the changes based on density, while ignoring driver sensitivity [40]. Based on driver sensitivity, the proposed system can characterize the traffic based on the driver conditions. Further, Refs. [18,49,51] consider a constant driver sensitivity, which cannot give accurate behavior. However, the proposed system based on the traffic variables used for the driver sensitivity can accurately devise traffic behavior. In other words, the proposed system can devised traffic behavior while considering the changes in headway and driver conditions. This gives more realistic and adequate traffic spatio-temporal evolution.

7. Conclusions

In this paper, a new macroscopic traffic system with driver sensitivity, transition distance, and safe distance headway is devised. The driver sensitivity is obtained from the equilibrium speed of the vehicles traversed over a road section. The proposed system contemplates traffic physics and practical parameters, whereas the PW system traffic considers a uniform constant velocity. It is ensured that the proposed traffic system is hyperbolic. The performance results depict that the proposed traffic system gives more appropriate and robust results than the PW traffic system. The transition in density and velocity evolution at changes in density and velocity are smooth and are within the employed range. In contrast, the PW traffic system has large variations at changes in velocity. The velocity even goes below zero and above the maximum limit. The results further showed that the proposed traffic system evolution with lower driver sensitivity evolves slowly and presents traffic congestion. Conversely, the traffic changes evolve quickly with higher driver sensitivity at traffic transitions and presents smooth flow. The proposed system can mitigate traffic and emissions and improve public safety. This system can also be used for traffic prediction and incorporation of road side limits. Further, this can be utilized for the smart road side units for connected and automated vehicles for efficient utilization of road infrastructure.

Author Contributions: Conceptualization, Z.H.K.; Methodology, Z.H.K.; Software, Z.H.K. and A.B.A.; Validation, Z.H.K.; Formal analysis, A.B.A.; Investigation, Z.H.K. and A.B.A., Z.H.K.; Writing—original draft, Z.H.K.; Writing—review & editing, Z.H.K. and A.B.A.; Visualization, Z.H.K.; Funding acquisition, A.B.A. All authors have read and agreed to the published version of the manuscript.

Funding: This research received no external funding.

Acknowledgments: The authors are thankful to W. Imran from the University of Naples, Federico II, Via Claudio 21, 80125, Naples, Italy for providing his valuable feedback.

Conflicts of Interest: The authors declare no conflict of interest.

References

1. Jiang, R.; Wu, Q.; Zhu, Z. A new continuum model for traffic flow and numerical tests. *Transp. Res. Part Methodol.* **2002**, *36*, 405–419. [CrossRef]
2. Kraft, B. Car Accidents Caused by Aggressive Driving. Kraft & Associates, 27-Feb-2023. Available online: https://www.kraftlaw.com/car-accidents/causes-car-accidents/car-accidents-caused-aggressive-driving/ (accessed on 25 April 2023).
3. Ai, W.H.; Wang, M.M.; Liu, D.W. Analysis of macroscopic traffic flow model considering throttle dynamics. *Eur. Phys. J.* **2023**, *96*. [CrossRef]
4. Khazini, L.; Kalajahi, M.J.; Blond, N. An analysis of emission reduction strategy for light and heavy-duty vehicles pollutions in high spatial–temporal resolution and emission. *Environ. Sci. Pollut. Res. Int.* **2022**, *29*, 23419–23435. [CrossRef] [PubMed]
5. Xu, C.; Liu, P.; Wang, W.; Li, Z. Identification of freeway crash-prone traffic conditions for traffic flow at different levels of service. *Transp. Res. Part Policy Pract.* **2014**, *69*, 58–70. [CrossRef]
6. Zhang, H.; Mine, T.; Ono, S.; Kawasaki, H. Analysis of the conditions for the occurrence of sudden braking using drive recorder videos: Using the distance between vehicles estimated by deep learning. *Seisan Kenkyu* **2022**, *74*, 129–134.
7. Shahariar, G.M.H.; Bodisco, T.A.; Zare, A.; Sajjad, M.; Jahirul, M.I.; Van, T.C.; Bartlett, H.; Ristovski, Z.; Brown, R.J. Impact of driving style and traffic condition on emissions and fuel consumption during real-world transient operation. *Fuel* **2022**, *319*, 123874. [CrossRef]
8. Knipling, R.R.; Mironer, M.; Hendricks, D.L.; Tijeripa, L.; Everson, J.; Allen, J.C.; Wilson, C.; Volpe, J.A. *Assessment of IVHS Countermeasures for Collision Avoidance: Rear-End Crashes*; DOT HS 807 995 Final Report; US Department of Transportation, National Highway Traffic Safety Administration: Washington, DC, USA, 1993.
9. Taieb-Maimon, M.; Shinar, D. Minimum and comfortable driving headways: Reality versus perception. *Hum. Factors J. Hum. Factors Ergon. Soc.* **2001**, *43*, 159–172. [CrossRef]
10. Borowsky, A.; Oron-Gilad, T.; Meir, A.; Parmet, Y. Drivers' perception of vulnerable road users: A hazard perception approach. *Accid. Anal. Prev.* **2012**, *44*, 160–166. [CrossRef]
11. Asadamraji, M.; Saffarzadeh, M.; Ross, V.; Borujerdian, A.; Ferdosi, T.; Sheikholeslami, S. A novel driver hazard perception sensitivity model based on drivers' characteristics: A simulator study. *Traffic Inj. Prev.* **2019**, *20*, 492–497. [CrossRef]
12. Meir, A.; Borowsky, A.; Oron-Gilad, T. Formation and evaluation of act and anticipate hazard perception training (AAHPT) intervention for young novice drivers. *Traffic Inj. Prev.* **2014**, *15*, 172–180. [CrossRef] [PubMed]
13. Constantinou, E.; Panayiotou, G.; Konstantinou, N.; Loutsiou-Ladd, A.; Kapardis, A. Risky and aggressive driving in young adults: Personality matters. *Accid. Anal. Prev.* **2011**, *43*, 1323–1331. [CrossRef]
14. Zhu, Y.; He, Z.; Sun, W. Network-wide link travel time inference using trip-based data from automatic vehicle identification detectors. *IEEE Trans. Intell. Transp. Syst.* **2020**, *21*, 2485–2495. [CrossRef]
15. Tang, K.; Chen, S.; Liu, Z. Citywide spatial-temporal travel time estimation using big and sparse trajectories. *IE Trans. Intell. Transp. Syst.* **2018**, *19*, 4023–4034. [CrossRef]
16. Treiber, M.; Hennecke, A.; Helbing, D. Congested traffic states in empirical observations and microscopic simulations. *Phys. Rev. E* **2000**, *62*, 1805–1824. [CrossRef]
17. Khan, D.; Khan, Z.H.; Imran, W.; Khattak, K.S.; Gulliver, T.A. Macroscopic flow characterization at T-junctions. *Transp. Res. Interdiscip. Perspect.* **2022**, *14*, 100591. [CrossRef]
18. Zhai, C.; Wu, W. A continuum model considering the uncertain velocity of preceding vehicles on Gradient Highways. *Phys. A Stat. Mech. Its Appl.* **2022**, *588*, 126561. https://doi.org.10.1016/j.physa.2021.126561. [CrossRef]
19. Heidemann, D. Some critical remarks on a class of traffic flow models. *Transp. Res. Part Methodol.* **1999**, *33*, 153–155. [CrossRef]
20. Newell, G.F. Nonlinear effects in the dynamics of car following. *Oper. Res.* **1961**, *9*, 209–229. [CrossRef]
21. Bando, M.; Hasebe, K.; Nakayama, A.; Shibata, A.; Sugiyama, Y. Dynamical model of traffic congestion and numerical simulation. *Phys. Rev. E.* **2000**, *51*, 1035–1042. [CrossRef]
22. Ali, F.; Khan, Z.H.; Khattak, K.S.; Gulliver, T.A. A microscopic traffic flow model characterization for weather conditions. *Appl. Sci.* **2022**, *12*, 12981. [CrossRef]
23. Helbing, D.; Tilch, B. Generalized force model of traffic dynamics. *Phys. Rev. E* **1998**, *58*, 133–138. [CrossRef]
24. Gipps, P.G. A behavioural car-following model for computer simulation. *Transp. Res. Part B* **1981**, *15*, 105–111.
25. Rahman, M.; Islam, M.R.; Chowdhury, M.; Khan, T. Development of a connected and automated vehicle longitudinal control model. *arXiv* **2020**, arXiv:2001.00135.
26. Treiber, M.; Kesting, A. *Traffic Flow Dynamics: Data, Models and Simulation*; Springer: Berlin, Germany, 2013. [CrossRef]
27. Cao, Z.; Lu, L.; Chen, C.; Chen, X.U. Modeling and simulating urban traffic flow mixed with regular and connected vehicles. *IEEE Access* **2021**, *9*, 10392–10399. [CrossRef] [PubMed]
28. Kesting, A.; Treiber, M.; Helbing, D. Enhanced intelligent driver model to access the impact of driving strategies on traffic capacity. *Philos. Trans. R. Soc. A Math. Phys. Eng. Sci.* **2010**, *368*, 4585–4605. [CrossRef]
29. Treiber, M.; Kesting, A.; Helbing, D. Delays, inaccuracies and anticipation in microscopic traffic models. *Phys. A Stat. Mech. Appl.* **2006**, *360*, 71–88. [CrossRef]

30. Li, Z.; Li, W.; Xu, S.; Qian, Y. Stability analysis of an extended intelligent driver model and its simulations under open boundary condition. *Phys. A Stat. Mech. Appl.* **2015**, *419*, 526–536.
31. Liebner, M.; Baumann, M.; Klanner, F.; Stiller, C. Driver intent inference at urban intersections using the intelligent driver mode. In Proceedings of the IEEE Intelligent Vehicle Symposium, Madrid, Spain, 3–7 June 2012. [CrossRef]
32. Nagel, K.; Wagner, P.; Woesler, R. Still flowing: Approaches to traffic flow and traffic jam modeling. *Oper. Res.* **2003**, *51*, 681–710.
33. Lighthill, M.; Whitham, G. On kinematic waves II. A theory of traffic flow on long crowded roads. *Proc. R. Soc. Lond. Ser. Math. Phys. Sci.* **1955**, *229*, 317–345. [CrossRef]
34. Richards, P. Shock waves on the highway. *Oper. Res.* **1956**, *4*, 42–51. [CrossRef]
35. Wierbos, M.J.; Knoop, V.L.; Hänseler, F.S.; Hoogendoorn, S.P. A macroscopic flow model for mixed bicycle-car traffic. *Transportmetrica* **2021**, *17*, 340–355. [CrossRef]
36. Daganzo, C.F. Requiem for second-order fluid approximations of traffic flow. *Transp. Res. Part Methodol.* **1955**, *29*, 277–286.
37. Maerivoet, S.; Moor, B.D. *Transportation Planning and Traffic Flow Models*; Katholieke Universiteit Leuven: Leuven, Belgium, 2008.
38. Payne, H.J. Models of Freeway Traffic and Control. *Math. Model. Public Syst. (Simul. Counc. Proc.)* **1971**, *1*, 51–61.
39. Whitham, G.B. *Linear and Nonlinear Waves*; Wiley: New York, NY, USA, 1971. [CrossRef]
40. Zhang, H. A theory of non-equilibrium traffic flow. *Transp. Res. Part Methodol.* **1998**, *32*, 485–498. [CrossRef]
41. Grace, M.; Potts, R. A theory of the diffusion of traffic platoons. *Oper. Res.* **1964**, *12*, 255–275.
42. Graham, E.F.; Chenu, D.C. A study of unrestricted platoon movement of traffic. *Traffic Eng.* **1962**, *32*, 11–13. [CrossRef]
43. Castillo, J.D.; Pintado, P.; Benitez, F. The reaction time of drivers and the stability of traffic flow. *Transp. Res. Part Methodol.* **1994**, *28*, 35–60. [CrossRef]
44. Aw, A.; Rascle, M. Resurrection of "second order" models of traffic flow. *Siam J. Appl. Math.* **2000**, *60*, 916–938.
45. Richardson, D.A. Refined Macroscopic Traffic Modelling via Systems of Conservation Laws. Masters' Thesis, Department of Mathematics and Statistics, University of Victoria, Victoria, BC, Canada, 2012. [CrossRef]
46. Phillips, W. A kinetic model for traffic flow with continuum implications. *Transp. Plan. Technol.* **1979**, *5*, 131–138. [CrossRef]
47. Papageorgiou, M. Some remarks on macroscopic traffic flow modelling. *Transp. Res. A* **1998**, *32*, 323–329. [CrossRef]
48. Gore, N.; Chauhan, R.; Easa, S.; Arkatkar, S. Traffic conflict assessment using macroscopic traffic flow variables: A novel framework for real-time applications. *Accid. Anal. Prev.* **2023**, *185*, 107020–107020. [CrossRef]
49. Zhang, H. Driver memory, traffic viscosity and a viscous vehicular traffic flow model. *Transp. Res. Part Methodol.* **2003**, *37*, 27–41. [CrossRef]
50. Zheng, L.; Jin, P.J.; Huang, H. An anisotropic continuum model considering bi-directional information impact *Transp. Res. Part Methodol.* **2015**, *75*, 36–57. [CrossRef]
51. Ge, H.X.; Cheng, R.J. The "backward looking" effect in the lattice hydrodynamic model. *Phys. A* **2008**, *387*, 6952–6958. [CrossRef]
52. Wang, Z., Ge, H.; Cheng, R. Nonlinear analysis for a modified continuum model considering driver's memory and backward looking effect. *Phys. Stat. Mech. Appl.* **2018**, *508*, 18–27. [CrossRef]
53. Jafaripournimchahi, A.; Cai, Y.; Wang, H.; Sun, L.; Tang, Y.; Babadi, A.A. A viscous continuum traffic flow model based on the cooperative car-following behaviour of connected and autonomous vehicles. *IET Intell. Transp. Syst.* **2023**, *17*, 973–991. [CrossRef]
54. Li, Y.; Chen, W.; Peeta, S.; He, X.; Zheng, T.; Feng, H. An extended microscopic traffic flow model based on the spring-mass system theory. *Mod. Phys. Lett. B* **2017**, *31*, 1750090.
55. Morgan, J.V. Numerical Methods for Macroscopic Traffic Models. Ph.D. Thesis, Department of Mathematics, University of Reading, Berkshire, UK, 2002. [CrossRef]
56. Toro, E.F.; Hidalgo, A.; Dumbser, M. Force schemes on unstructured meshes I: Conservative hyperbolic systems. *J. Comput. Phys.* **2009**, *228*, 3368–3389.
57. Kachroo, P.P.E.; Wadoo, S.A.; Al-nasur, S.J.; Shende, A. Numerical Methods. In *Pedestrian Dynamics Feedback Control of Crowd Evacuation*; Kachroo, P.P.E., Wadoo, S.A., Al-nasur, S.J., Shende, A., Eds.; Springer: New York, NY, USA, 2008; pp. 61–93. [CrossRef]
58. Khan, Z.; Gulliver, T.A. A macroscopic traffic model based on transition velocities. *J. Comput. Sci.* **2020**, *43*, 101131. https://doi.org/10.1016/j.jocs.2020.101131.
59. Moura, C.A.D.; Kubrusly, C.S. *The Courant–Friedrichs–Lewy (CFL) Condition: 80 Years After Its Discovery*; Springer: Berlin, Germany, 2013.
60. Ni, D. *Traffic Flow Theory*; Elsevier: Amsterdam, The Netherlands, 2016; pp. 55–58. [CrossRef]
61. Weik, N. Macroscopic traffic flow in railway systems—A discussion of the applicability of fundamental diagrams. *J. Rail Transp. Plan. Manag.* **2002**, *23*, 100330. [CrossRef]
62. Mararo, L.E. A macroscopic fundamental diagram for spatial analysis of traffic flow: A case study of Nyeri town, Kenya. *Am. J. Civ. Eng.* **2015**, *3*, 150–156. [CrossRef]
63. Daganzo, C.F.; Geroliminis, N. An analytical approximation for the macroscopic fundamental diagram of urban traffic. *Transp. Res. Part B Methodol.* **2008**, *42*, 771–781.
64. Daganzo, C.F.; Li, Y.; Gonzales, E.J.; Geroliminis, N. *City-Scale Transport Modeling: An Approach for Nairobi, Kenya*; Institute of Transportation Studies, University of California Berkeley: Berkeley, CA, USA, 2007.

65. Basak, K.; Hetu, S.N.; Azevedo, C.L.; Loganathan, H.; Toledo, T.; Runminxu; Yanxu; Li-Shiuanpeh; Ben-Akiva, M. Modeling reaction time within a traffic simulation model. In Proceedings of the International IEEE Conference on Intelligent Transportation Systems, Hague, The Netherlands, 6–9 October 2013; pp. 302–309. [CrossRef]
66. Ngoduy, D.; Tampere, C. Macroscopic effects of reaction time on traffic flow characteristics. *Phys. Scr.* **2009**, *80*, 025802. [CrossRef]
67. Yi, P.; Lu, J.; Zhang, Y.; Lu, H. Safety-based capacity analysis for Chinese highways. *IATSS Res.* **2004**, *28*, 47–55.